

MSc Module MTMM14:

Numerical modelling of atmospheres and oceans

More advanced spatial schemes

4.1 Series expansion methods

4.2 Lagrangian and semi-lagrangian schemes

Course content

Week 1: The Basics

- 1.1 Introduction
- 1.2 Brief history of numerical weather forecasting and climate modelling
- 1.3 Dynamical equations for the unforced fluid

Week 2: Modelling the real world

- 2.1 Physical parameterisations: horizontal mixing and convection
- 2.2 Ocean modelling

Week 3: Staggered schemes

- 3.1 Staggered time discretisation and the semi-implicit method
- 3.2 Staggered space discretisations

Week 4: More advanced spatial schemes

- 4.1 Lagrangian and semi-lagrangian schemes
- 4.2 Series expansion methods:
finite element and spectral methods

Week 5: Synthesis

- 5.1 Revision
- 5.2 Test

4.1 Lagrangian schemes

Key idea

Move the grid with the flow so that there is no longer any advection term and hence advective CFL instability can be avoided (\rightarrow so larger time steps can be used).

- Frames of reference
- 1-dimensional example
- Good points and bad points of the method

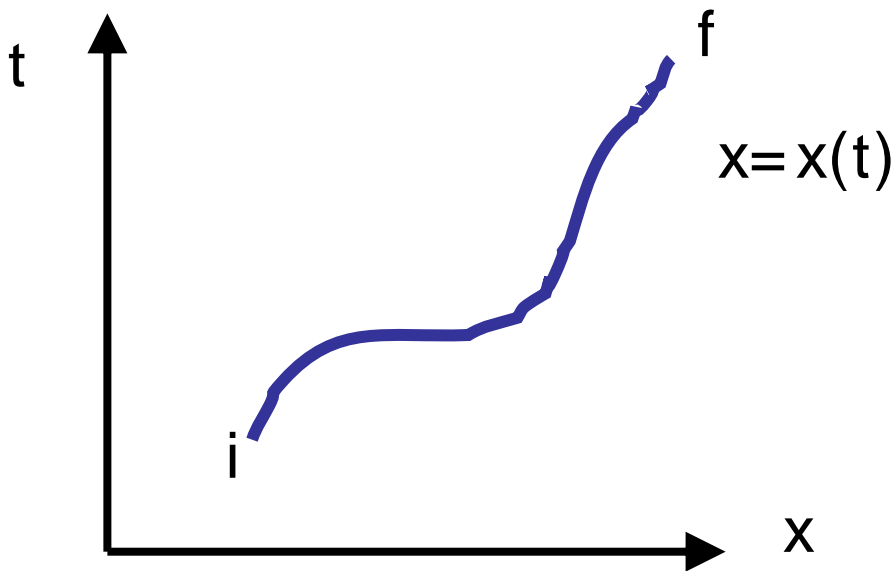
4.1 Frames of reference



- Eulerian – coordinate system geographically fixed (e.g. latitude-longitude coordinates).
- Lagrangian – coordinate system moves with the fluid.

Grid points in fully Lagrangian schemes get advected along by the flow – therefore no explicit advection term in the equations. However, grid becomes horribly distorted and non-linear stability is likely to occur.

4.1 1-dimensional example



$$\frac{D\xi}{Dt} = \frac{\partial \xi}{\partial t} + u \frac{\partial \xi}{\partial x} = F$$

$$\xi_f - \xi_i = \int_{x(t)} \frac{\partial \xi}{\partial t} dt + \frac{\partial \xi}{\partial x} dx$$

$$= \int_{x(t)} \left(F - u \frac{\partial \xi}{\partial x} \right) dt + \frac{\partial \xi}{\partial x} dx$$

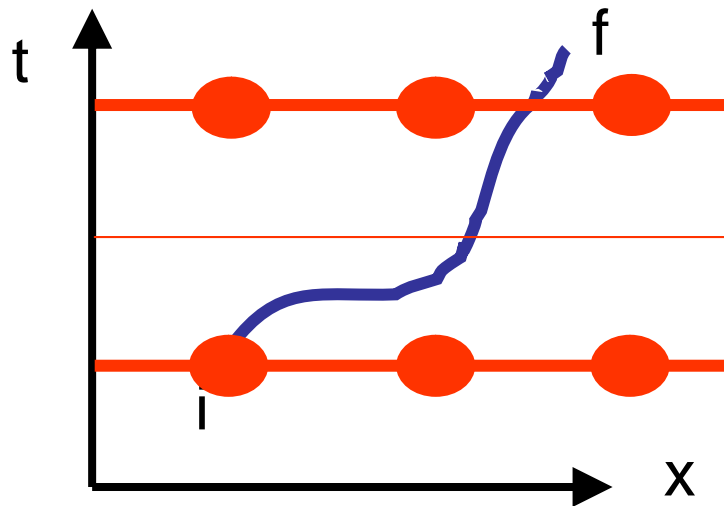
$$= \int_{x(t)} \left(\frac{\partial \xi}{\partial x} \right) (dx - \dot{x} dt) + \int_{x(t)} F dt$$

■ Eulerian: $dx - u dt = -u dt$

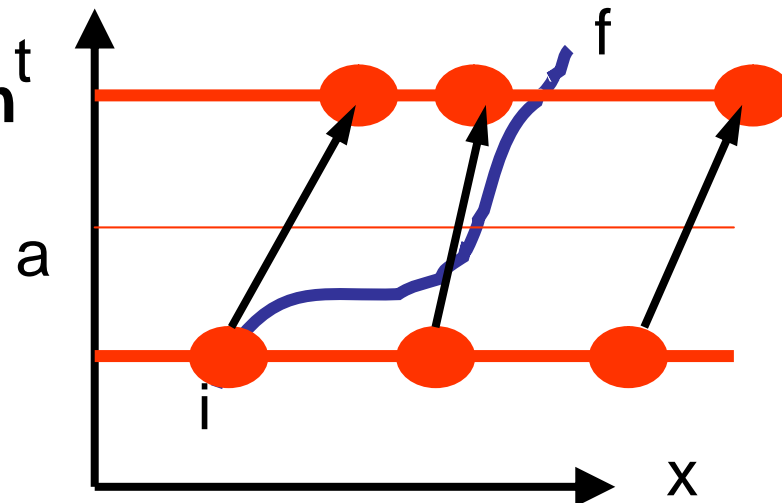
■ Lagrangian: $dx - u dt = 0$

4.1 Eulerian and Lagrangian schemes

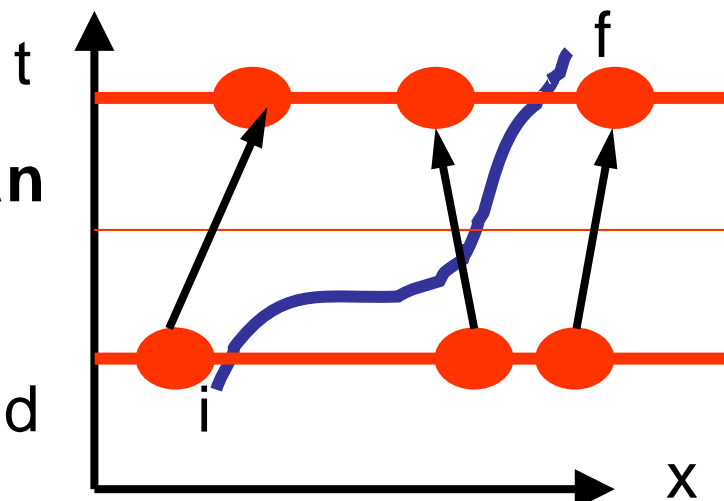
Eulerian
grid points
don't move



Lagrangian
grid points
advect from a
regular grid



Semi-Lagrangian
grid points
advect onto
a regular grid



4.1 Semi-Lagrangian

$$\xi(x_i^{n+1}) - \xi(\tilde{x}_i^n) = \oint_{x(t)} F dt$$

Steps:

- Back trajectory calculation to find out where grid point was on previous time step e.g. $\tilde{x}_i^n = x_i^n - u_i^{n+1} h$
- Find the field at this location by interpolating the field from neighbouring grid points (e.g. cubic interpolation)
- Find the integrated forcing by using numerical quadrature (e.g. Simpson's rule over a half time step).

4.1 Semi-lagrangian

Advantages:

- No advection term
- No advective CFL problems so time step can be larger (→ less time steps needed)
- Less problems with the pole

Disadvantages:

- Have to calculate a back trajectory for each grid point at each time step
- More CPU needed per time step
- Problems with fast forcing (e.g. doppler shift of gravity waves over mountains)
- Overly diffusive on low resolution grids

Example:

Ritchie et al. 1995 ECMWF

$h=3\text{mins}$ (Eulerian) → 15 mins (Semi-Lagr)

SL takes 20% more CPU per step so net speed up is factor of 4.

4.1 Summary of main points

- Once gravity waves have been slowed down using semi-implicit schemes, the maximum time step is determined by advective CFL
- Lagrangian methods can be used to remove the advection term and so avoid these CFL limits
- Semi-lagrangian is better than Lagrangian because it results in a regular grid on the new time step
- Time step is then determined by accuracy requirements rather than by stability limitations.

4.2 Series expansion (Galerkin) methods

Key idea –

use a finite set of spatial basis functions to represent the spatial variation (rather than a finite set of grid point variables).

- Finite difference schemes
- Finite volume schemes
- Galerkin methods:
 - Finite element
 - Spectral

4.2 Reduction of truncation error

Consider the PDE $L[u]-g=0$ which has true solution u . $L[.]$ is a non-linear differential operator and g is some forcing function. The numerical solution u^* satisfies $L[u^*]-g=e$ where e is the residual truncation error.

Three main classes of method:

1. **Point collocation** – set e to zero only at specific locations (grid points).
2. **Least squares** – minimise e^*e averaged over the whole domain
3. **Galerkin** – set e to be orthogonal to the set of pre-defined spatial basis functions.

$$\int \Phi_i(x)e(x,t)dA = 0$$

http://www.cs.ut.ee/~toomas_/linalg/dv/node1.html

4.2 Finite volume schemes

Advection term can be written in different ways:

$$\begin{aligned}u \cdot \nabla \xi &\rightarrow u_{ij} (\xi_{i+1,j} - \xi_{i-1,j}) + v_{ij} (\xi_{i,j+1} - \xi_{i,j-1}) \\ \nabla \cdot (u \xi) &\rightarrow (u_{i+1,j} \xi_{i+1,j} - u_{i-1,j} \xi_{i-1,j}) + (v_{i,j+1} \xi_{i,j+1} - v_{i,j-1} \xi_{i,j-1}) \\ k \cdot \nabla \times (u \times \xi k) &\rightarrow ???\end{aligned}$$

1st form is known as “advection form”

2nd form is known as “flux form”

When equations are solved in flux form, the total flux of vorticity into grid cells is conserved. Rather than thinking of **finite differences** one is thinking of **finite volumes**.

Equal combination of all 3 forms gives what is known as the **Arakawa jacobian** – which conserves energy and enstrophy. (→ hence more stable!!).

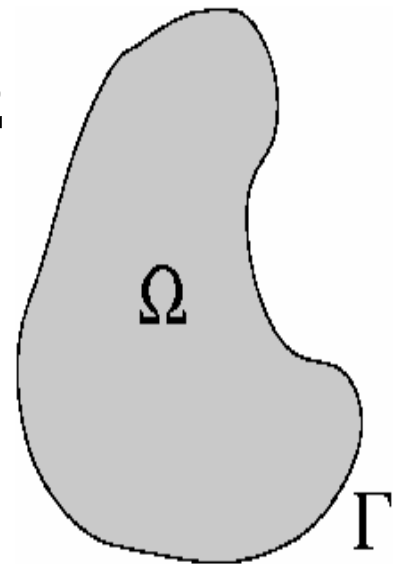
4.2 Integral formulation of a PDE

Example: diffusion equation

$$\frac{\partial \xi}{\partial t} = \nabla \cdot (\kappa \nabla \xi)$$

Equivalent “*weak form*” integral formulation:

$$\begin{aligned} \frac{\partial}{\partial t} \int_{\Omega} w \xi \, d\Omega &= \int_{\Omega} w \nabla \cdot (\kappa \nabla \xi) \, d\Omega \\ &= - \int_{\Omega} \kappa \nabla w \cdot \nabla \xi \, d\Omega \end{aligned}$$

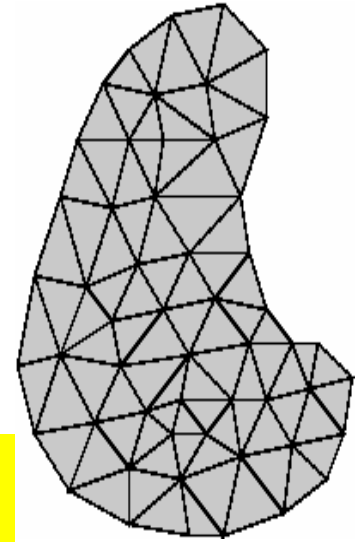


where w is an arbitrary *weight (test) function*

4.2 The Galerkin finite element method

Divide the domain into a finite set of N elements. Then approximate the solution as:

$$\xi(t, \mathbf{x}) = \sum_{i=1}^N \hat{\xi}_i(t) \Phi_i(\mathbf{x})$$



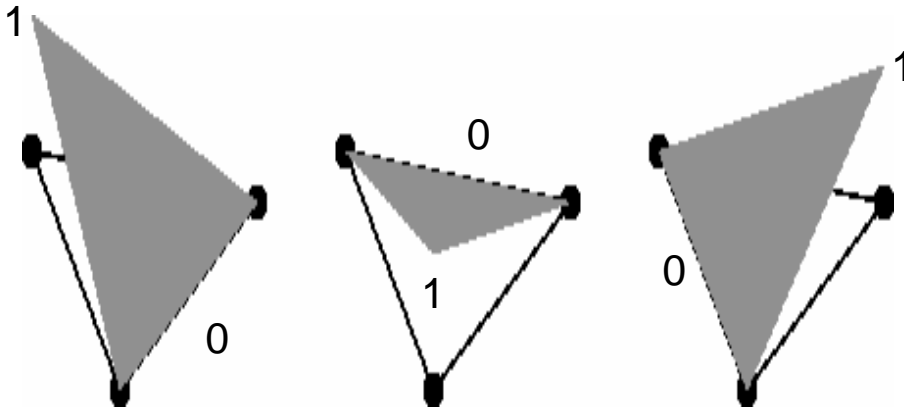
Where the Φ_i are the **basis functions** at node i .

$$\sum_{i=1}^N \Phi_i(\mathbf{x}) = 1$$

Solve weak form of the equations for finite series of test functions, w_i

Galerkin method: choose $w_i = \Phi_i$

4.2 Example: basis functions for linear elements



Higher-order (e.g., quadratic) elements
=> more nodes

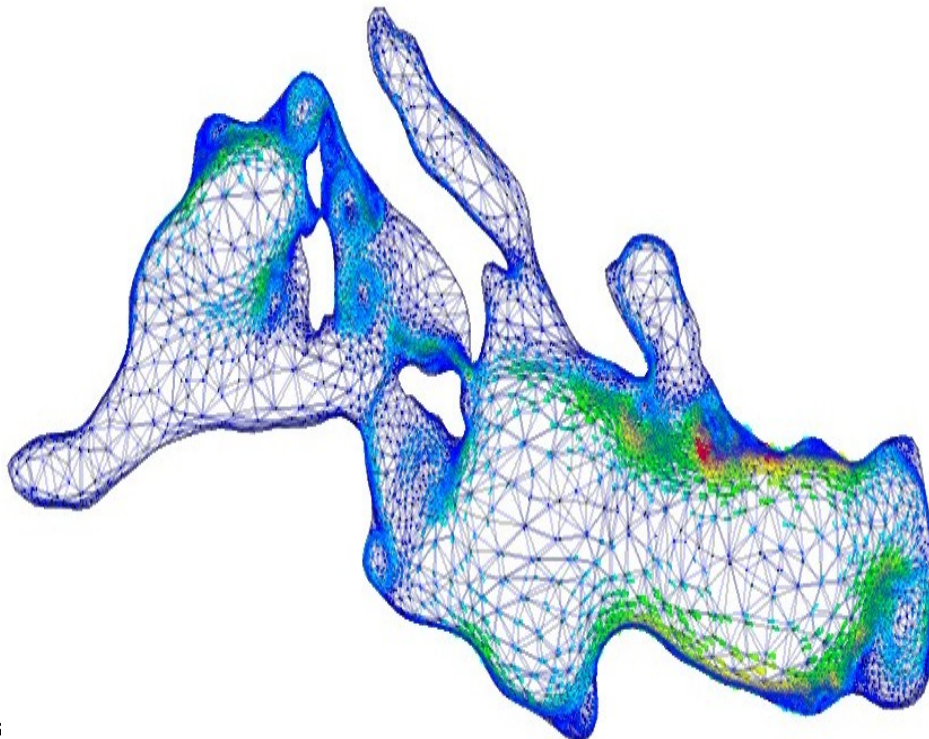
While higher-order elements are nominally more accurate, when combined with adaptive meshing, low-order elements offer maximum flexibility (for fixed computational resources) and the errors can be rigorously controlled

4.2 Example: ICOM

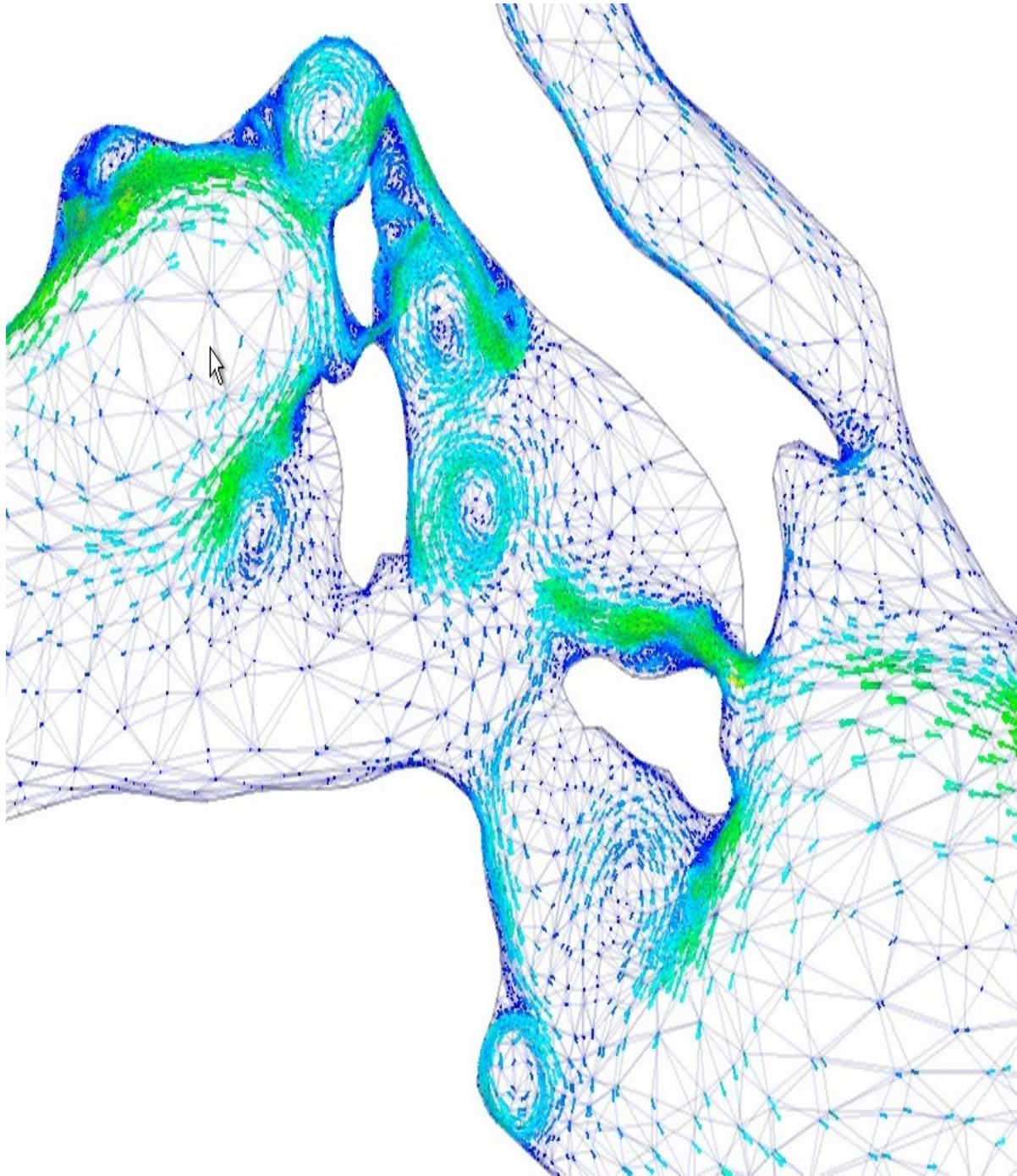
Imperial College Ocean Model

David Marshall (University of Reading), Chris Pain, Matthew Piggott, Philip Power, Adrian Umpleby, Matthew Eaton, Gerard Gorman, Cassiano de Oliveira, Tony Goddard (Imperial College, London)

- General-purpose code for solving 3-D Navier-Stokes equations that incorporates unstructured meshing with dynamic mesh adaptivity;
- Need to solve a 4th-order elliptic problem - currently use a conjugate-gradient solver (to be replaced by multigrid solver). Domain decomposition methods employed for parallel processors.
- Initially approx. 1/4 degree everywhere:



4.2 Adapted mesh



Nodes \approx 25,000

Elements \approx 65,000

4.2 Pros and cons of FE schemes

Advantages of finite element schemes:

- can conform very accurately to the basin geometry;
- various 'natural' boundary conditions can be included in a very straightforward manner;
- formulation based on rigorous mathematical foundations, allowing statements about errors, convergence to be made.

HOWEVER finite-element methods are more computationally expensive than finite-difference methods, but some of this can be offset by adaptive meshing:

- remeshing controlled by a functional that gauges the quality of the mesh, based on the Hessian of the velocity/tracer fields and prescribed error tolerances;
- constraints on aspect ratio of elements and size variations between adjacent elements and prescribed minimum and maximum element size.

4.2 Spectral methods

Key idea

Use basis functions that are eigensolutions of the spatial derivative operators

e.g. Fourier modes:

$$\Phi = e^{i(kx+ly)}$$
$$\Rightarrow \frac{\partial \Phi}{\partial x} = ik\Phi$$

- Perfectly accurate derivatives
Note: ik not $2i\sin(kd)$
- Very simple Laplacian terms
- Nice smooth solutions (continuous differentiable)

4.2 1-d example

$$\frac{\partial \xi}{\partial t} + u \frac{\partial \xi}{\partial x} - \kappa \frac{\partial^2 \xi}{\partial x^2} = 0$$

$$\xi(x, t) = \sum_{k=1}^N \xi_k(t) e^{i2\pi kx/N}$$

$$\Rightarrow \frac{d\xi_k}{dt} + \sum_{j=1}^N \frac{2\pi j}{N} u_{k-j} \xi_j + \kappa \left(\frac{2\pi k}{N} \right)^2 \xi_k = 0$$

- PDE converted into a set of N ODEs – one for each Fourier mode amplitude
- Diffusion term is very simple – just a wavenumber dependent damping for each Fourier mode
- Advection term consists of non-linear triad interaction between mode amplitudes
- Method takes $O(N^2)$ CPU operations rather than $O(N)$ for finite difference so becomes prohibitive for large N!

4.2 The transform method

Fast Fourier Transform (FFT) algorithm $O(N \log N)$ rather than $O(N^2)$ operations

Carl Friedrich Gauss, "Nachlass: Theoria interpolationis methodo nova tractata," *Werke* band **3**, 265–327 (Königliche Gesellschaft der Wissenschaften, Göttingen, 1866). See also M. T. Heideman, D. H. Johnson, and C. S. Burrus, "Gauss and the history of the fast Fourier transform," *IEEE ASSP Magazine* **1** (4), 14–21 (1984).

James W. Cooley and John W. Tukey, "An algorithm for the machine calculation of complex Fourier series," *Math. Comput.* **19**, 297–301 (1965).

The Transform Method

- Calculate du/dx etc. in wavenumber space
- Transform them to physical space by FFT
- Multiply them together to get advection terms
- Inverse FFT back to wavenumber space

$O(N \log N)$ rather than $O(N^2)$ → speed up of 20 ($N=100$) 145 ($N=1000$)

Orszag, S. A., 1970:

Transform method for the calculation of vector-coupled sums:
Application to the spectral form of the vorticity equation. *J. Atmos. Sci.*, **27**, 890-895.

4.2 The ECMWF spectral model

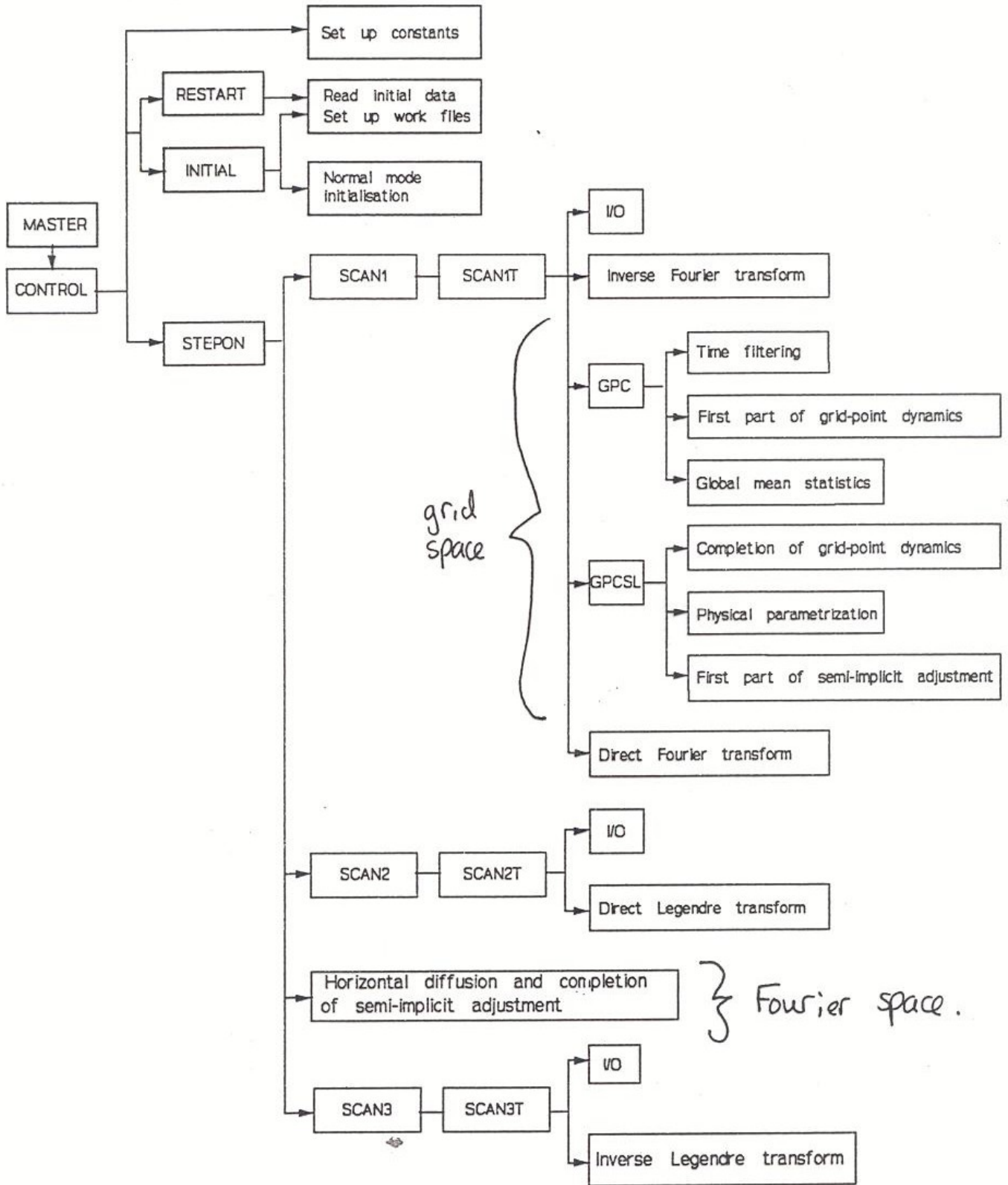


Fig. 1.2 Simplified flow diagram of the ECMWF forecast model

4.2 Spectral methods in GCMs

The spectral technique has become the most widely used method of integrating the governing equations of numerical weather prediction over hemispheric or global domains.

Following the development of efficient transform methods by Orszag (1970) and Eliassen *et al.* (1970), and the construction and testing of multi-level primitive-equation models (e.g. Bourke, 1974; Hoskins and Simmons, 1975; Daley *et al.*, 1976), spectral models were introduced for operational forecasting in Australia and Canada during 1976. The technique has been used operationally in the USA since 1980, in France since 1982, and in Japan and at ECMWF since 1983. The method is also extensively used by groups involved in climate modelling.

Comprehensive accounts of the technique are given by Machenhauer (1979), and Jarraud and Simmons (1984).

4.2 Spectral methods on the sphere

On a flat 2-dimensional domain we could use Fourier modes:

$$\xi(x, y, t) = \sum_{k,l} \xi_{kl}(t) e^{i(kx+ly)}$$

BUT the Earth isn't flat and so these are eigensolutions of the Laplacian operator on the sphere. So instead need to use surface harmonics (spherical harmonics):

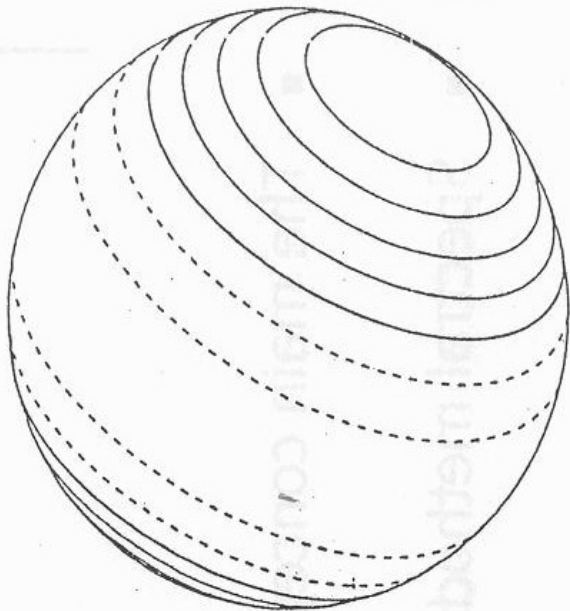
$$\xi(x, \sin \theta, t) = \sum_n \sum_m \xi_{mn}(t) Y_n^m(x, \sin \theta)$$

$$Y_n^m(x, \sin \theta) = e^{imx} P_n^m(\sin \theta)$$

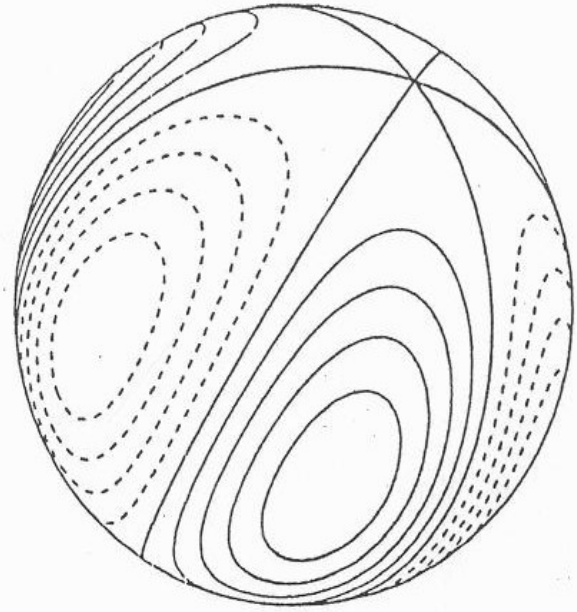
- n =truncation
- m =zonal wavenumber $|m| \leq n$
- Fourier mode in x -direction (in longitude)
- Associated Legendre polynomial in latitude direction with $n-|m|$ zeros between poles

4.2 Some spherical harmonics

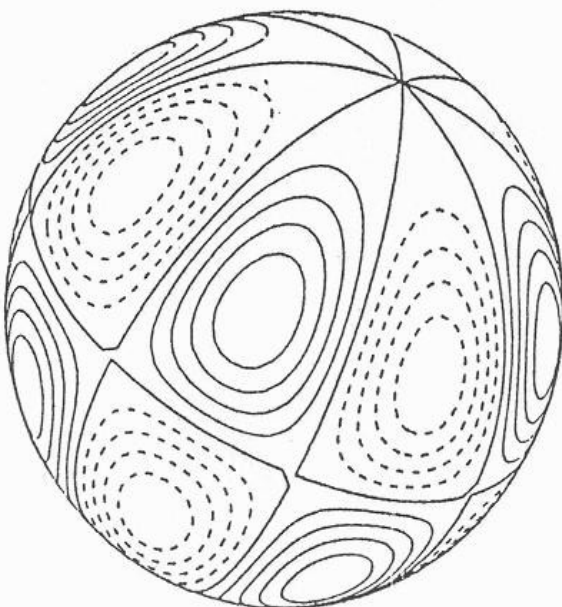
$\text{Re } Y_2^0$



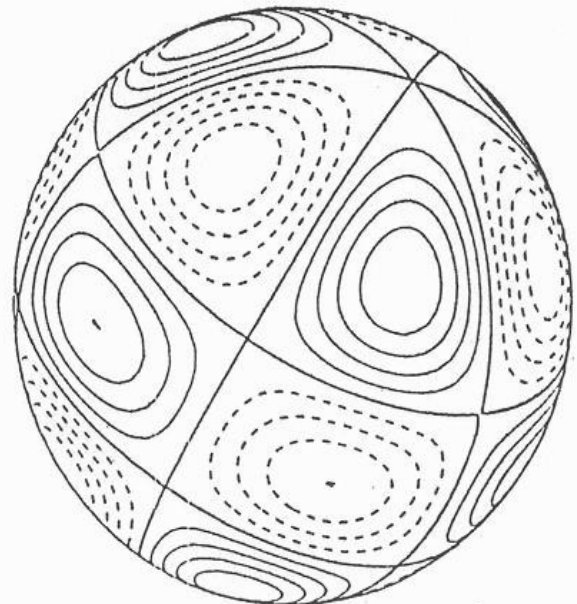
$\text{Re } Y_3^3$



$\text{Re } Y_5^4$



$\text{Re } Y_5^3$



4.2 Some definitions and properties

$$P_n^m(y) = \sqrt{\frac{(2n+1)(n-m)!}{2(n+m)!}} \frac{(1-y^2)^{m/2}}{2^n n!} \frac{d^{n+m}}{dy^{n+m}} (y^2-1)^n$$

⇒

$$P_0^0 = \frac{1}{\sqrt{2}}$$

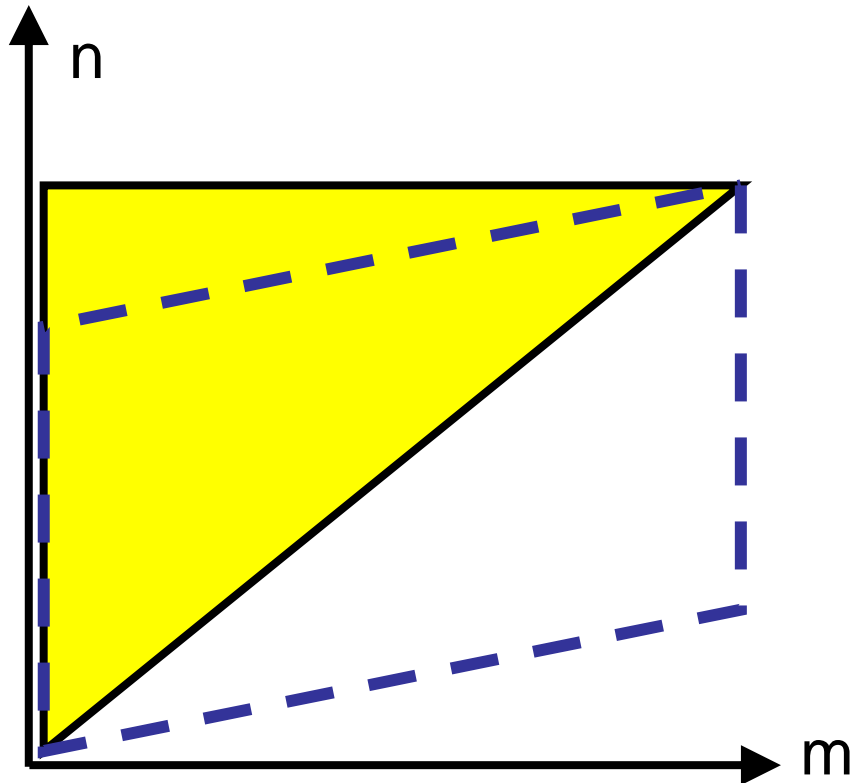
$$P_1^0 = y\sqrt{\frac{3}{2}} \quad P_1^1 = \sqrt{\frac{3(1-y^2)}{4}}$$

$$P_2^0 = (3y^2-1)\sqrt{\frac{5}{8}} \quad P_2^1 = y\sqrt{1-y^2}\sqrt{\frac{15}{4}} \quad P_2^2 = 1-y^2\sqrt{\frac{15}{16}}$$

$$\frac{1}{4\pi} \int_0^{2\pi} \int_{-1}^1 Y_{n'}^{m'*} Y_n^m dy dx = \begin{cases} 1 & m'=m \quad n'=n \\ 0 & \text{otherwise} \end{cases}$$

$$\nabla^2 Y_n^m = \frac{-n(n+1)}{a^2} Y_n^m$$

4.2 Truncation and resolution



Two types of truncation:

Triangular e.g. T42

Rhomboidal e.g. R15

Triangular gives isotropic resolution whereas rhomboidal gives more resolution meridionally

T42 means maximum number of waves

around equator $m=42 \rightarrow$

resolution $\sim 0.5 * 360\text{deg}/42 \sim 4.3$ degrees

The resolution of global spectral models

René Laprise

*Physics Department, University of Québec at Montréal
Montréal, Quebec, Canada*

The letter of Professor Pielke (1991) suggesting a definition of horizontal resolution of gridpoint models prompts me to reciprocate with a short essay on a corresponding analysis for global spectral models. The horizontal structure of dependent variables in spectral models is represented by series expansion of spherical harmonics Y_n^m , where $0 \leq |m| \leq n$ (e.g., Kubota 1959); the transform method (Machenhauer and Rasmussen 1972) is used to calculate nonlinear terms on a Gaussian latitude-longitude grid in all modern spectral models. Triangular truncation ($0 \leq n \leq N$) of the series is often used, as it offers uniform resolution on a spherical domain. As this note will try to show, there does not seem to be any straightforward way to define an equivalent mesh size for spectral models; this makes the estimation of effective resolution even more difficult than in gridpoint models.

A sometimes quoted estimate of spectral-model resolution consists in the average spacing between Gaussian latitudes of the transform grid; for triangular truncation, this spacing is equal to that between longitudes at the equator: $L_1 \approx 2\pi a / (3N + 1)$, with a the radius of the earth. Hence, $L_1 \approx 13.3/N$ in units of thousands of kilometers; for a T31 model, $L_1 = 426$ km. This estimate of resolution is overly optimistic because the dimensions of the transform grid are chosen to allow calculation of quadratic terms without aliasing of the resolved spectral fields, and hence the transform grid is finer than required by the information content of the corresponding spectral series.

A more realistic estimate of resolution is given by the size of half a wavelength of the shortest resolved zonal wave at the equator: $L_2 = \pi a / N \approx 20/N$ in units of thousands of kilometers. Hence, a T31 model would have a resolution of $L_2 = 646$ km, according to this measure. Triangular truncation provides an isotropic and uniform resolution on a sphere. The shortest resolved zonal wave ($|m| = N$) used to determine L_2 corresponds to a mode with the gravest meridional

structure, because modes that are very short in one direction must be elongated in the other direction: sectorial spherical harmonics ($|m| = n$) have modal structures shaped as orange segments and have their largest amplitude in the tropics, hardly an adequate measure of resolution for general circulation models.

An alternative way to estimate the resolution of spectral models is as follows. Consider that the area of the earth's surface is given by $4\pi a^2$; there are $(N + 1)^2$ real coefficients to a spherical harmonic series at triangular truncation with maximum index N , that is, $N(N + 1)/2$ complex coefficients for the modes $1 \leq |m| \leq N$, plus $(N + 1)$ real coefficients for the modes with $m = 0$. If an equal area on the surface of the earth is assigned to every piece of information contained in the series, this gives a footprint of surface area equal to $4\pi a^2 / (N + 1)^2$ for every real coefficient. Resolution in a spectral model could be defined as the width L_3 of a flat, rectangular tile of the same surface area: $L_3 = (4\pi)^{1/2} a / (N + 1) \approx 22.6/N$ in units of thousands of kilometers. Hence, a T31 model would have a resolution of $L_3 = 728$ km, according to this measure.

Yet another definition of resolution for spectral models would be to consider the representative spatial dimension of high-order tesseral harmonics ($0 < |m| < n = N$). The eigenvalue of the Laplacian operator applied on a spherical harmonics Y_n^m is $-K^2 \equiv -n(n + 1)/a^2$. Equating the eigenvalue of the highest resolved mode with the corresponding eigenvalue of Fourier modes in Cartesian geometry for the purpose of estimating resolution gives: $K^2 = N(N + 1)/a^2 = k_x^2 + k_y^2$. Considering modes with unity aspect ratio, $k_x^2 = k_y^2 = k^2$, that is, with checkerboard-like modal structure, gives $k^2 = N(N + 1)/(2a^2)$. An alternative measure of resolution would be one-half of the corresponding wave-length: $L_4 \equiv \pi/k \approx 2^{1/2} \pi a / N \approx 28.3/N$ in units of thousands of kilometers. So for a T31 model, $L_4 = 899$ km.

It is noteworthy that the estimates of resolution given by L_2 , L_3 , and L_4 are all coarser than the simple-minded, overly optimistic estimate given by L_1 . Pielke's

remarks about the “effective” resolution of finite-difference models being coarser than the mesh size also apply to spectral models to some extent. It would be naive to think that the effective resolution of a spectral model is defined by even the most pessimistic of the estimates suggested above. Even though the Galerkin formalism of spectral models removes the numerical approximations associated with the horizontal discretization in finite-difference models, time-discretization errors and aliasing in the calculation of some of the terms, especially in the parameterization of physical effects, are unavoidable. Also, the horizontal dissipation that is applied to the upper part of the spectrum to prevent “spectral blocking” effectively reduces the information content below its theoretical limit given by the spectral truncation. For example, even the most scale-selective formulation suggested by Leith (e.g., Boer et al. 1984) substantially damps the upper 20% part of the resolved spectrum in low-resolution versions; other formulations, such as har-

monic or biharmonic diffusion, are even less scale selective. Therefore any of the aforementioned definitions of L must be viewed simply as upper limits to the effective resolution of a spectral model for a given truncation.

References

- Boer, G.J., N.A. McFarlane, R. Laprise, J.D. Henderson, and J.-P. Blanchet, 1984: The Canadian Climate Centre spectral atmospheric general circulation model. *Atmos.–Ocean*, **22**(4), 397–429.
- Kubota, S., 1959: Surface spherical harmonic representations of the system of equations for analysis. *Papers in Meteor. and Geophys.*, **X**(3), 145–166.
- Machenhauer, B., and E. Rasmussen, 1972: On the integration of the spectral hydrodynamical equations by a transform method. Kobenhavns Universitet, Institut for Teoretisk Meteorologi, Copenhagen, Rep. No. 3, 44 pp.
- Pielke, R.A., 1991: A recommended specific definition of “resolution.” *Bull. Amer. Meteor. Soc.*, **72**(12), 1914.

Some disadvantages of spherical harmonics:

- more CPU time needed per time step
- not local so can generate non-local artefacts such as Gibbs oscillations
- not clear what resolution they resolve

A. Navarra, W.F. Stern and K. Miyakoda, 1994:

Reduction of the Gibbs Oscillation in Spectral Model Simulations
Journal of Climate: Vol. 7, No. 8, pp. 1169–1183.

Lander, J. and Hoskins, B. J. (1997).

Believable scales and parameterizations in a spectral transform met
Monthly Weather Review, **125**, 292-303.

4.2 Summary of main points

- Finite differences are a rather naïve way of solving PDEs
- Better approach is to use a set of spatial basis functions – either local piecewise functions (Finite Elements) or harmonics (Spectral methods)
- These methods generally take more computer time per time step but can achieve more accurate results